Magnetic ordering in $Gd_2Sn_2O_7$: the archetypal Heisenberg pyrochlore antiferromagnet

2006 J. Phys.: Condens. Matter 18 L37

(http://iopscience.iop.org/0953-8984/18/3/L02)

INSTITUTE OF PHYSICS PUBLISHING JOURNAL OF PHYSICS: CONDENSED MATTER

J. Phys.: Condens. Matter **18** (2006) L37–L42 doi:10.1088/0953-8984/18/3/L02

LETTER TO THE EDITOR

Magnetic ordering in $Gd_2Sn_2O_7$: the archetypal Heisenberg pyrochlore antiferromagnet

A S Wills[1,2], M E Zhitomirsky[3], B Canals[4], J P Sanchez[3], P Bonville[5], P Dalmas de Réotier[3] and A Yaouanc[3]

[1] Department of Chemistry, University College London, 20 Gordon Street, London WC1H 0AJ, UK
[2] Davy-Faraday Research Laboratory, The Royal Institution of Great Britain, London W1S 4BS, UK
[3] Commissariat à l'Energie Atomique, DSM/DRFMC/SPSMS, 38054 Grenoble, France
[4] Laboratoire Louis Néel, CNRS, BP-166, 38042 Grenoble, France
[5] Commissariat à l'Energie Atomique, DSM/SPEC, 91191 Gif-sur-Yvette, France

Received 18 November 2005
Published 6 January 2006
Online at stacks.iop.org/JPhysCM/18/L37

Abstract

Low-temperature powder neutron diffraction measurements are performed in the ordered magnetic state of the pyrochlore antiferromagnet $Gd_2Sn_2O_7$. Symmetry analysis of the diffraction data indicates that this compound has the ground state predicted theoretically for a Heisenberg pyrochlore antiferromagnet with dipolar interactions. The difference in the magnetic structure of $Gd_2Sn_2O_7$ and of nominally analogous $Gd_2Ti_2O_7$ is found to be determined by a specific type of third-neighbour superexchange interaction on the pyrochlore lattice between spins across empty hexagons.

(Some figures in this article are in colour only in the electronic version)

Frustration, or the inability to simultaneously satisfy all independent interactions [1], has become an important theme in condensed matter research, coupling at the fundamental level a wide range of phenomena such as high-T_c superconductivity, the folding of proteins and neural networks. Magnetic crystals provide one of the simplest stages within which to explore the influence of frustration, particularly when it arises as a consequence of lattice geometry rather than due to disorder. For this reason, geometrically frustrated magnetic materials have been the object of intense scrutiny for over 20 years [2]. Particular interest has been focused on *kagomé* and *pyrochlore* (see figure 1) geometries of vertex-sharing triangles and tetrahedra respectively. Model materials with their structures display a wide range of exotic low-temperature physics, such as spin ice [3], spin liquids [4], topological spin glasses [5], heavy fermion [6] and cooperative paramagnetic ground states [7]. Research into these systems was spawned from studies of the archetypal geometrically frustrated system, namely the Heisenberg pyrochlore antiferromagnet, which in the classical limit was shown theoretically to possess a disordered ground state. Raju and co-workers found that the Heisenberg pyrochlore antiferromagnet with dipolar interactions has an infinite number of degenerate spin configurations near the mean-field

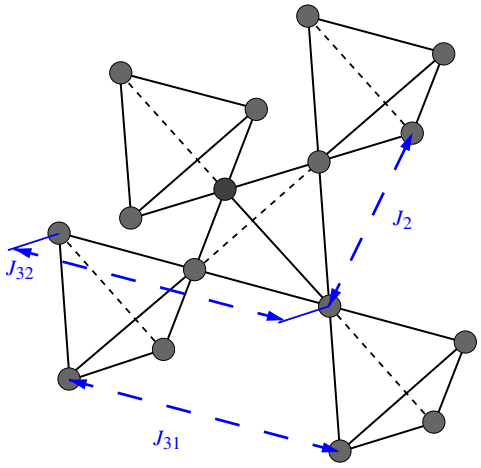

Figure 1. Pyrochlore lattice of vertex-sharing tetrahedra. Next-neighbour exchanges are shown by long-dashed lines.

transition temperature, which are described by propagation vectors [*hhh*] [8]. Later, Palmer and Chalker showed that quartic terms in the free energy lift this degeneracy and stabilize a four-sublattice state with the ordering vector $\mathbf{k} = (0\,0\,0)$ (the PC state) [9].

Among various pyrochlore materials $Gd_2Ti_2O_7$ and $Gd_2Sn_2O_7$ are believed to be good realizations of Heisenberg antiferromagnets. Indeed, the Gd^{3+} ion has a half-filled 4f-shell with nominally no orbital moment. However, a strong *intrashell* spin–orbit coupling mixes $^8S_{7/2}$ and $^6P_{7/2}$ states, leading to a sizable crystal-field splitting. Recent electron spin resonance (ESR) measurements on dilute systems gave comparable ratios of the single-ion anisotropy constant $D > 0$ to the nearest-neighbour exchange J for the two compounds: $D/J \sim 0.7$ [10]. This corresponds to a planar anisotropy for the ground state. Magnetic properties of the stannate and the titanate would therefore be expected to be very similar. In this light, the contrasts between the low-temperature behaviour of $Gd_2Sn_2O_7$ and that of the analogous titanate are remarkable. While the titanate displays two magnetic transitions, at $\sim$0.7 and 1 K, to structures with the ordering vector $\mathbf{k} = \left(\frac{1}{2}\,\frac{1}{2}\,\frac{1}{2}\right)$ [11, 12], the stannate undergoes a first-order transition into an ordered state near 1 K [13]. Furthermore, Mössbauer measurements indicate that in the latter the correlated Gd^{3+} moments still fluctuate as $T \to 0$ K [14].

In this letter we demonstrate that $Gd_2Sn_2O_7$ orders with the PC ground state, evidence for an experimental realization of a Heisenberg pyrochlore antiferromagnet with dipolar interactions. We also note that the magnetic structure observed in $Gd_2Sn_2O_7$ differs from those observed in the closely related $Gd_2Ti_2O_7$, indicating that an extra interaction is at play in the latter which leads to the observed differences.

In order to reduce the absorption of neutrons, a 500 mg sample of $Gd_2Sn_2O_7$ enriched with ^{160}Gd was prepared following the conditions given in [13]. Powder neutron diffraction spectra were collected with neutrons of wavelength 2.4 Å using the D20 diffractometer of the Institute Laue-Langevin, Grenoble at two temperatures below $T_N = 1$ K (0.1 and 0.7 K), as well as one temperature in the paramagnetic phase above T_N (1.4 K). Due to the high residual absorption of the Gd sample, extended counting times of 5 h per temperature were required. The magnetic contribution to diffraction at 0.1 K could be well isolated from scattering by the cryostat walls and dilution insert by subtraction of the spectrum at 1.4 K. Symmetry calculations were made using SARA*h* [15] and Rietveld refinement of the diffraction data using Fullprof [16] together with SARA*h*.

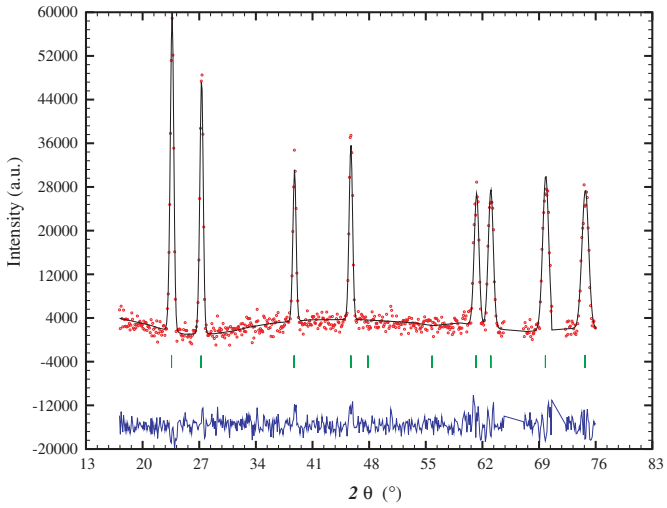

Figure 2. Fit to the magnetic diffraction pattern of $Gd_2Sn_2O_7$ obtained from the ψ_6 basis state by Rietveld refinement. The dots correspond to experimental data obtained by subtraction of that measured in the paramagnetic phase (1.4 K) from that in the magnetically ordered phase (0.1 K). The solid line corresponds to the theoretical prediction and the line below to the difference. Positions for the magnetic reflections are indicated by vertical markers.

The magnetic diffraction peaks, figure 2, can be indexed with the propagation vector $\mathbf{k} = (0\,0\,0)$. The different types of magnetic structure can be classified in terms of the irreducible co-representations of the reducible magnetic co-representation, $c\Gamma_{\rm mag}$. In the case of $Gd_2Sn_2O_7$ (space group $Fd\bar{3}m$ with $\mathbf{k} = (0\,0\,0)$ and a Gd^{3+} ion at the 16d crystallographic position) this can be written as: $c\Gamma_{\rm mag} = 1c\Gamma_{3+} + 1c\Gamma_{5+} + 1c\Gamma_{7+} + 2c\Gamma_{9+}$ [17][6]. Their associated basis vectors are represented in figure 3. Inspection reveals that $c\Gamma_{3+}$ corresponds to the antiferromagnetic structure observed in FeF_3 [18], $c\Gamma_{5+}$ to the linear combination observed in the model XY pyrochlore antiferromagnet $Er_2Ti_2O_7$ [11], $c\Gamma_{7+}$ to the manifold of states proposed as the ground states for the Heisenberg pyrochlore antiferromagnet with dipolar terms (the PC ground state) and $c\Gamma_{9+}$ to a spin-ice like manifold observed in the non-collinear ferromagnetic pyrochlores such as $Dy_2Ti_2O_7$ [3]. While the phase transition in $Gd_2Sn_2O_7$ has been shown to be first order, which allows ordering according to several irreducible co-representations, it is commonly found that the terms which drive the transition to being first order are relatively weak and cause only minor perturbation to the resultant magnetic structure. Following this, we examined whether the models detailed above could fit the observed magnetic neutron diffraction spectrum. The goodness of fit parameter, χ^2, for the fit to models characterized by each irreducible co-representation are: $c\Gamma_{3+}$ (69.0), $c\Gamma_{5+}$ (35.6), $c\Gamma_{7+}$ (5.18), $c\Gamma_{9+}$ (13.6). We find that the magnetic scattering can only be well modelled by $c\Gamma_{7+}$, the PC state in which the moments of a given Gd tetrahedron are parallel to the tetrahedron's edges. In this state each moment is fixed to be perpendicular to the local three-fold axis of each tetrahedron, consistent with Mössbauer data [13, 14]. Powder averaging leads to the structures ascribed to ψ_4, ψ_5 and ψ_6 being indistinguishable by neutron

[6] The co-representations are real and are labelled according to the notation of Kovalev [17] for the parent representation and whether the antiunitary halfing group was created according to $d(a) = \pm\delta(aa_0^{-1})\beta$, where $d(a)$ is the matrix representative of the antiunitary symmetry element a, $\delta(aa_0^{-1})$ is the matrix representative of the unitary symmetry element aa_0^{-1}, a_0 is an antiunitary generating element and β is an unitary matrix.

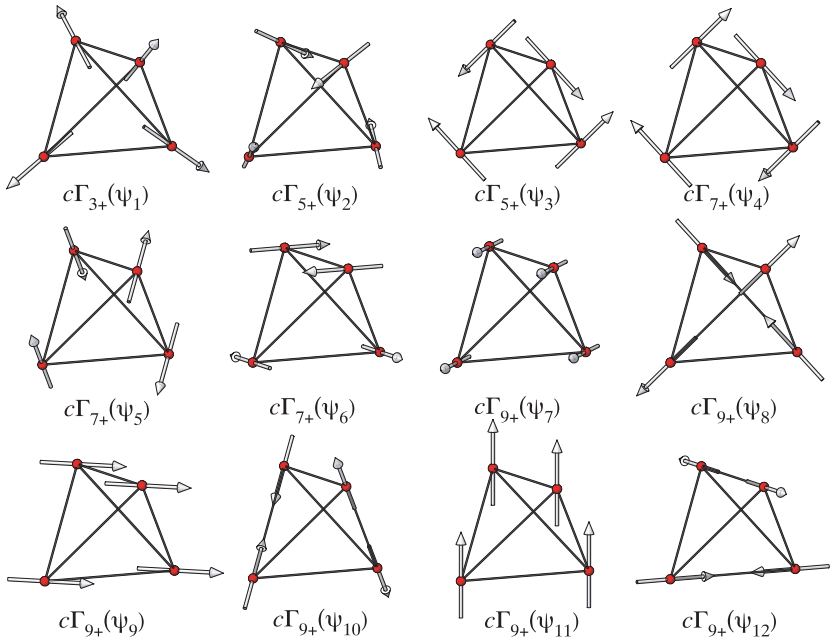

Figure 3. The magnetic structure basis vectors labelled according to the different irreducible co-representations for $Gd_2Sn_2O_7$.

diffraction and prevents contributions of the individual basis vectors from being refined. For this reason only ψ_6 was used in the refinement and the final fit is presented in figure 2. While the value of the ordered moment, 6(1) μ_B/Gd^{3+}, obtained by scaling the magnetic and nuclear peaks is imprecise due to the uncertainty over the isotopic composition of the Gd and the concomitant neutron absorption, it is consistent with the free-ion value (7 μ_B) and that measured by Mössbauer spectroscopy [13].

Realization of the PC state in $Gd_2Sn_2O_7$, but not in $Gd_2Ti_2O_7$, indicates that the magnetic Hamiltonian of the titanate contains additional terms. Cépas and Shastry [19] have suggested that next-neighbour exchange may stabilize magnetic ordering at $\mathbf{k} = (\frac{1}{2}\,\frac{1}{2}\,\frac{1}{2})$, though the corresponding region in the parameter space was found to be tiny. Also, possible exchange paths were not investigated in their work as both types of third-neighbour exchange (figure 1) were assumed to be equal.

The pyrochlore $A_2B_2O_7$ structure has two inequivalent oxygen sites: O1 at $(x, \frac{1}{8}, \frac{1}{8})$ and O2 at $(\frac{3}{8}, \frac{3}{8}, \frac{3}{8})$. The oxygen parameter is $x = 0.335$ and 0.326 for the stannate and the titanate, respectively [20]. Using this information we have determined that the nearest-neighbour gadolinium ions are connected with short Gd–O1(2)–Gd bonds. The second-neighbour exchange J_2 is produced by two distinct Gd–O1–O1–Gd bridges. The O1–O1 distance in the first path is 2.63 Å with two equal bond angles of 118°. In the second path, |O1–O1| = 3.04 Å, the angles are 148° and 98°. (Distances and angles are given for $Gd_2Ti_2O_7$.)

There are two types of third-neighbour pairs in the pyrochlore lattice indicated in figure 1 as J_{31} and J_{32}, which correspond to three- and two-step Manhattan (city-block) distances, respectively. The superexchange J_{31} is determined by two equivalent Gd–O1–O1–Gd paths with |O1–O1| = 3.04 Å and two equal angles of 148°. The superexchange J_{32} is produced by

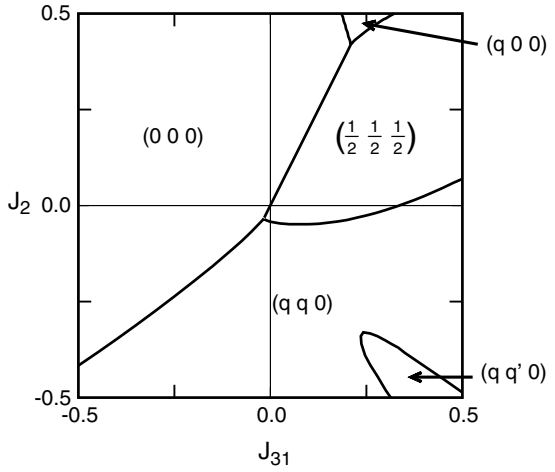

Figure 4. Instability wavevectors for different values of second- and third-neighbour exchange constants for a Heisenberg pyrochlore antiferromagnet with dipolar interactions. Incommensurate states are indicated by non-zero components of the wavevectors. All transition lines are of the first-order.

two Gd–O1–O2–Gd bridges with a significantly larger interoxygen distance |O1–O2| = 3.62 Å and bond angles of 152° and 143°. As a result, the two exchange constants for third-neighbour pairs have to be different with $J_{32} \ll J_{31}$. The Goodenough–Kanamori–Anderson rules also suggest that the second-neighbour constant J_2 must be smaller than J_{31} since bond angles in the corresponding superexchange paths are significantly closer to 90°. Similar relations should hold for next-neighbour exchange constants in $Gd_2Sn_2O_7$ with, perhaps, a somewhat larger ratio J_2/J_{31} due to a larger angle 126° in the second-neighbour superexchange path. The overall effect of further neighbour exchange is, however, reduced in the stannate because of a larger lattice constant $a = 10.45$ Å compared with $a = 10.17$ Å in the titanate [20].

Next, we consider the following Hamiltonian:

$$\hat{\mathcal{H}} = \sum_{\langle i,j\rangle} J_{ij}\mathbf{S}_i \cdot \mathbf{S}_j + D\sum_i (\mathbf{n}_i \cdot \mathbf{S}_i)^2 + (g\mu_B)^2 \sum_{\langle i,j\rangle}\left[\frac{\mathbf{S}_i \cdot \mathbf{S}_j}{r_{ij}^3} - \frac{3(\mathbf{S}_i \cdot \mathbf{r}_{ij})(\mathbf{S}_j \cdot \mathbf{r}_{ij})}{r_{ij}^5}\right],$$

where the superexchange J_{ij} extends up to the third-neighbour pairs of spins and $D > 0$ is a single-ion anisotropy. The strength of the dipolar interaction between nearest-neighbour spins $E_{dd} = (g\mu_B)^2/(a\sqrt{2}/4)^3$ is estimated as $E_{dd}/J \approx 0.2$ for the titanate [8], where J is the nearest-neighbour exchange constant (in the following $J \equiv 1$). Applying mean-field theory [8, 19] and evaluating dipolar sums via Ewald's summation we have determined the instability wavevector for different values of second- and third-neighbour exchange constants. Results are essentially independent of the anisotropy constant $D > 0$ since the dipolar interaction already selects spins to be orthogonal to the local trigonal axes $\mathbf{n}_i$ for the eigenstates with the highest transition temperature.

If only the nearest-neighbour exchange is present, in agreement with previous works [8, 19] we find an approximate degeneracy of modes along the cube diagonal with a very shallow minimum ∼0.5% at $\mathbf{k} = (\frac{1}{2}\,\frac{1}{2}\,\frac{1}{2})$. In such a case, a fluctuation-driven first-order transition is expected to the PC state [9, 21]. The diagram of possible ordering wavevectors for a restricted range of J_{31} and J_2 is presented in figure 4. It contains two commensurate states with $\mathbf{k} = (0\,0\,0)$ and $\mathbf{k} = (\frac{1}{2}\,\frac{1}{2}\,\frac{1}{2})$ and three incommensurate phases. Remarkably, already weak *antiferromagnetic* J_{31} robustly stabilizes the $\mathbf{k} = (\frac{1}{2}\,\frac{1}{2}\,\frac{1}{2})$ magnetic structure, which exists in a

wide range $0 < J_{31} < 0.335J$. In contrast, a small *ferromagnetic* J_2 within a narrow window $-0.04J < J_2 < 0$ is needed to obtain the same ordering without J_{31}. In the whole range of parameters, the eigenstate with $\mathbf{k} = (\frac{1}{2}\,\frac{1}{2}\,\frac{1}{2})$ corresponds to a 120° spin structure with $q = 0$ in the transverse kagomé plane with zero ordered moment on interstitial sites. The only remaining degeneracy corresponds to a four-fold orbit of the $\mathbf{k} = (\frac{1}{2}\,\frac{1}{2}\,\frac{1}{2})$ vector.

We have also verified that the second type of third-neighbour exchange J_{32} does not lead to further stabilization of the $(\frac{1}{2}\,\frac{1}{2}\,\frac{1}{2})$ spin structure. Based on these results and the above analysis of the exchange paths we conclude that it is the third-neighbour exchange across empty hexagons J_{31} (figure 1) which is responsible for the magnetic structure observed in $Gd_2Ti_2O_7$ [11, 12]. In $Gd_2Sn_2O_7$ further neighbour exchanges play a less significant role due to a larger lattice constant and, in addition, the ratio J_2/J_{31} might be enhanced due to somewhat different bond angles such that it lies closer to the transition boundary between $\mathbf{k} = (0\,0\,0)$ and $(\frac{1}{2}\,\frac{1}{2}\,\frac{1}{2})$ states.

In conclusion, the occurrence of the PC state in $Gd_2Sn_2O_7$ but not in $Gd_2Ti_2O_7$ indicates that the latter possesses additional contributions, which we identify as a type of third-neighbour exchange. $Gd_2Sn_2O_7$ therefore presents the only accurate realization of a Heisenberg pyrochlore antiferromagnet with dipolar interactions.

We are grateful to A Forget for preparing the ^{160}Gd-enriched sample and to the ILL for provision of neutron time. ASW would like to thank the Royal Society and EPSRC (grant number EP/C534654) for financial support.

References

[1] Anderson P W 1973 *Mater. Res. Bull.* **8** 153
[2] Villain J 1979 *Z. Phys.* B **33** 31
[3] Harris M J, Bramwell S T, McMorrow D F, Zeiske T and Godfrey K W 1997 *Phys. Rev. Lett.* **79** 2554
[4] Ballou R, Lelièvre-Berna E and Fåk B 1996 *Phys. Rev. Lett.* **77** 790
[5] Wills A S, Depuis V, Vincent E and Calemczuk R 2000 *Phys. Rev.* B **62** 9264(R)
[6] Urano C, Nohara M, Kondo S, Sakai F, Takagi H, Shiraki T and Okubo T 2000 *Phys. Rev. Lett.* **85** 1052
[7] Gingras M J P, den Hertog B C, Faucher M, Gardner J S, Dunsiger S R, Chang L J, Gaulin B D, Raju N P and Greedan J E 2000 *Phys. Rev.* B **62** 6496
[8] Raju N P, Dion M, Gingras M J P, Mason T E and Greedan J E 1999 *Phys. Rev.* B **59** 14489
[9] Palmer S E and Chalker J T 2000 *Phys. Rev.* B **62** 488
[10] Glazkov V N, Zhitomirsky M E, Smirnov A I, Krug von Nidda H-A, Loidl A, Marin C and Sanchez J P 2005 *Phys. Rev.* B **72** 020409(R)
Glazkov V N, Smirnov A I, Sanchez J P, Forget A, Colson D and Bonville P 2005 *Preprint* cond-mat/0510575
[11] Champion J D M, Wills A S, Fennell T, Bramwell S T, Gardner J S and Green M A 2001 *Phys. Rev.* B **64** 140407
[12] Stewart J R, Ehlers G, Wills A S, Bramwell S T and Gardner J S 2004 *J. Phys.: Condens. Matter* **16** L321
[13] Bonville P, Hodges J A, Ocio M, Sanchez J P, Vulliet P, Sosin S and Braithwaite D 2003 *J. Phys.: Condens. Matter* **15** 7777
[14] Bertin E, Bonville P, Bouchaud J-P, Hodges J A, Sanchez J P and Vulliet P 2002 *Eur. Phys. J.* B **27** 347
[15] Wills A S 2000 *Physica* B **276** 680
progam available from ftp.ill.fr/pub/dif/sarah/
[16] Rodriguez-Carvajal J 1993 *Physica* B **192** 55
[17] Kovalev O V 1993 *Representations of the Crystallographic Space Groups* 2nd edn (Switzerland: Gordon and Breach)
[18] Greedan J E, O'Reilly A H and Stager C V 1987 *Phys. Rev.* B **35** 8770
[19] Cépas O and Shastry B M 2004 *Phys. Rev.* B **69** 184402
[20] Kennedy B J, Hunter B A and Howard C J 1997 *J. Solid State Chem.* **130** 58
Helean K B, Ushakov S V, Brown C E, Navrotsky A, Lian J, Ewing R C, Farmer J M and Boatner L A 2004 *J. Solid State Chem.* **177** 1858
[21] Brazovskii S A 1975 *Zh. Eksp. Teor. Fiz.* **68** 175
Brazovskii S A 1975 *Sov. Phys.—JETP* **41** 85 (Engl. Transl.)
Cepas O, Young A P and Shastry B S 2005 *Phys. Rev.* B **72** 184408